

# Null Geodesics of Charged Black Holes in String Theory

Sharmanthie Fernando <sup>1</sup>  
*Department of Physics & Geology*  
*Northern Kentucky University*  
*Highland Heights*  
*Kentucky 41099*  
*U.S.A.*

## Abstract

In this paper we investigate the null geodesics of the static charged black hole in heterotic string theory. A detailed analysis of the geodesics are done in the Einstein frame as well as in the string frame. In the Einstein frame, the geodesics are solved exactly in terms of the Jacobi-elliptic integrals for all possible energy levels and angular momentum of the photons. In the string frame, the geodesics are presented for the circular orbits.

*Key words:* Static, Charged, Heterotic, Black Holes, Geodesics, Strings

## 1 Introduction

String theory has become the leading candidate to unify gravity with the rest of the fundamental forces in nature. Therefore, studies of black holes in string theory takes an important place in current research. In this paper, we wish to study four dimensional spherically symmetric static charged black holes in heterotic string theory. The action of the low-energy heterotic string theory in four dimensions is given as follows,

$$S = \frac{1}{16\pi} \int d^4x \sqrt{-\det g} \left( R - \frac{1}{12} e^{-4\Phi} H_{\mu\nu\rho} H^{\mu\nu\rho} - 2(\nabla\Phi)^2 - e^{-2\Phi} F_{\mu\nu} F^{\mu\nu} \right) \quad (1)$$

Here  $g_{\mu\nu}$  is the metric,  $F_{\mu\nu} = \partial_\mu A_\nu - \partial_\nu A_\mu$  is the field strength corresponding to the Maxwell field  $A_\mu$ ,  $\Phi$  is the dilaton field, and,

$$H_{\mu\nu\rho} = \partial_\mu B_{\nu\rho} + \text{cyclic permutations} - (\Omega_3(A))_{\mu\nu\rho} \quad (2)$$

where  $B_{\mu\nu}$  is an antisymmetric tensor gauge field. The gauge Chern-Simons term is given as,

$$(\Omega_3(A))_{\mu\nu\rho} = \frac{1}{4} (A_\mu F_{\nu\rho} + \text{cyclic permutations}) \quad (3)$$

---

<sup>1</sup>fernando@nku.edu

For more details, see[1][2].

In this paper, we will focus on the solution to the action in eq.(1) with the fields  $H_{\mu\nu\alpha}$  and  $B_{\mu\nu}$  set to zero. Hence the heterotic string action simplifies to,

$$S = \frac{1}{16\pi} \int d^4x \sqrt{-g} \left[ R - 2(\nabla\Phi)^2 - e^{-2\Phi} F_{\mu\nu} F^{\mu\nu} \right] \quad (4)$$

Here  $\Phi$  is the dilaton field,  $R$  is the scalar curvature and  $F_{\mu\nu}$  is the Maxwell's field strength. The static charged black hole solutions to the above action were found first by Gibbons and Maeda[3]. It was also independently found by Garfinkle, Horowitz and Strominger [4] few years later. In the rest of the paper, we will refer to this black hole as the Gibbons-Maeda-Garfinkle-Horowitz-Strominger (GMGHS) black hole.

The main objective of this paper is to study the geodesic structure of massless particles of the GMGHS black hole. Studies of test particles, both massive and massless is one way to understand the gravitational field around a black hole. Since the motion of test particles around black holes are determined by the geodesic structure, a detailed analysis of geodesics are of great significance. Theoretical predictions such as light deflection, gravitational time-delay, perihelion shift and Lense-Thirring effect etc are physical elements that can be compared with observations when one study black holes in the universe. All of such phenomenon are related to the geodesics of black holes. Furthermore, the study of orbits of test particles is of astrophysical relevance when it comes to flow of particles in accretion disks around black holes.

Geodesics of black holes are studied extensively in the literature. There are many works related to the geodesics of well known charged black hole in general relativity which is the Reissner-Nordström black hole. Pugliese et.al.[5][6] have studied the geodesics of neutral as well as charged test particles of the Reissner-Nordström black hole recently. Analytical solutions of the electrically and magnetically charged test particles were discussed by Grunau and Kagramanova[7]. Chandrasekhar[8] and Hackmann et.al.[9] also have studied the geodesics of the Reissner-Nordström black hole.

There are few works that we like to mention that have addressed geodesics related to string black holes. Kinematics of the time-like geodesic congruences of string black holes in two and four dimensions were discussed by Dasgupta et.al in[10]. Motion of test particles around a charged dilatonic black hole is discussed by Maki and Shiraishi [11]. Hidden symmetries, null geodesics and photon capture of the Sen black hole, which is the rotating version of the GMGHS black hole, is discussed by Hioki and Miyamoto[12]. There, comments of the circular photon orbits of the GMGHS black hole are given. Bounded radial geodesics of the Sen black hole is discussed by Baga and Baga[13]. Gravitational lensing by a charged black hole in string theory was studied by Bhadra[14]. The geodesics of the 2+1 dimensional string black hole was studied by Fernando et.al[15].

The paper is organized as follows. In section 2, we will present the GMGHS black hole in the Einstein frame and string frame. A comparison with the Reissner-Nordström black hole is included in this section. The geodesic equations for the

GMGHS black hole in the Einstein frame is derived in section 3. A detailed discussion of the null geodesics in the Einstein frame follows in section 4. In section 5, the geodesic equations in string frame is presented. The null geodesics in string frame is discussed in section 6. Finally, the conclusion is given in section 7.

## 2 The GMGHS charged black hole in string theory

### 2.1 GMGHS black hole in Einstein frame

The GMGHS black hole solution to the action in eq.(4) is given by,

$$ds_E^2 = - \left(1 - \frac{2M}{r}\right) dt^2 + \frac{1}{\left(1 - \frac{2M}{r}\right)} dr^2 + r \left(r - \frac{Q^2}{M}\right) (d\theta^2 + \sin^2(\theta) d\phi^2) \quad (5)$$

Here, the electric field strength and the dilaton field are given by,

$$F_{rt} = \frac{Q}{r^2}; \quad e^{2\Phi} = 1 - \frac{Q^2}{Mr} \quad (6)$$

In the  $r - t$  plane, the metric simplifies to,

$$ds_E^2 = - \left(1 - \frac{2M}{r}\right) dt^2 + \frac{1}{\left(1 - \frac{2M}{r}\right)} dr^2 \quad (7)$$

Hence, the metric is identical to the Schwarzschild black hole metric. There is an event horizon at  $r = 2M$ . However, the area of the sphere of the string black hole is smaller and the area approaches zero when  $r = Q^2/M$ . Therefore,  $r = Q^2/M$  surface is singular. For  $Q^2 \leq M$ , the singular surface is inside the event horizon and the Penrose diagram is identical to the Schwarzschild black hole. See the review on black holes by Townsend[16] for more details about the Schwarzschild black hole. When  $Q^2 = 2M^2$ , the singular surface coincide with the horizon. This is the extremal limit where a transition between the black hole and the naked singularity occurs.

### 2.2 GMGHS black hole in string frame

In the above presentation of the GMGHS black hole, we have written it in the so-called ‘‘Einstein frame’’. In Einstein frame, the action is the Einstein-Hilbert action that is used in general relativity. However, when dealing with low-energy string theory and its solutions, there is another frame called ‘‘string frame’’ in which the metric can be written. String frame is some times preferred because it is the metric that strings directly coupled to. Which frame is more suitable to describe the current state of the universe is an open question which needs to be settled by experiments. An interesting

discussion on the relations between the string frame and the Einstein frame is given by Casadio and Harms[17].

The two metrics are related to each other by a conformal transformation given by,

$$g_{\mu\nu}^E = e^{-2\Phi} g_{\mu\nu}^S \quad (8)$$

which will lead to,

$$ds_{string}^2 = -\frac{\left(1 - \frac{2m}{r}\right)}{\left(1 + \frac{2m \sinh^2(\alpha)}{r}\right)^2} dt^2 + \frac{dr^2}{\left(1 - \frac{2m}{r}\right)} + r^2(d\theta^2 + \sin^2(\theta)d\phi^2) \quad (9)$$

The physical mass  $M$  and the charge  $Q$  are related to  $m$  and  $\alpha$  as,

$$M = m \cosh^2(\alpha), \quad Q = \sqrt{2}m \sinh(\alpha) \cosh(\alpha) \quad (10)$$

Note that the horizon in the string frame is

$$r_h^{string} = 2m = \frac{2M}{\cosh^2(\alpha)} \quad (11)$$

Since  $\cosh(\alpha) \geq 1$ , the horizon in the string frame is smaller than the one in the Einstein frame with the same mass. Therefore, the black hole seems “smaller” in string frame.

### 2.3 Comparison of the GMGHS black hole with the Reissner-Nordström black hole

The well known charged black hole in Einstein-Maxwell gravity is given by,

$$ds_E^2 = -\left(1 - \frac{2M}{r} + \frac{Q^2}{r^2}\right) dt^2 + \frac{1}{\left(1 - \frac{2M}{r} + \frac{Q^2}{r^2}\right)} dr^2 + r^2 d\Omega^2 \quad (12)$$

This metric has mass  $M$  and charge  $Q$  and have two horizons,

$$r_{\pm} = \frac{M \pm \sqrt{M^2 - Q^2}}{2} \quad (13)$$

Reissner-Nordström black hole become a naked singularity when  $Q^2 = M^2$ .

In comparison with the GMGHS black hole, there are similarities as well as differences. Both represents black holes for small  $Q/M$  and become naked singularities for large  $Q/M$ . The GMGHS black hole lack inner horizon while the Reissner-Nordström black hole does. For both solutions, maximal value of charge exists to separate black hole from the naked singularity. However, the extrem solutions do have different properties[4]. More details comparing the GMGHS black hole to Reissner-Nordström black hole and to the Schwarzschild black hole can be found in the paper by Garfinkle et.al.[4] and the review by Horowitz[18].

### 3 Geodesics in Einstein Frame

First we will derive the geodesic equations for neutral particles around the GMGHS black hole. We will follow the same approach given in the well known book by Chandrasekhar[8]. The metric is written as,

$$ds^2 = -f(r)dt^2 + f(r)^{-1}dr^2 + R(r)^2(d\theta^2 + \sin^2(\theta)d\phi^2) \quad (14)$$

Here,

$$f(r) = \left(1 - \frac{2M}{r}\right) \quad (15)$$

$$r \left(r - \frac{Q^2}{M}\right) = r(r - a) \quad (16)$$

and,

$$a = \frac{Q^2}{M} \quad (17)$$

Equations governing the geodesics in this space-time can be derived from the Lagrangian equation,

$$\mathcal{L} = -\frac{1}{2} \left( -f(r) \left(\frac{dt}{d\tau}\right)^2 + \frac{1}{f(r)} \left(\frac{dr}{d\tau}\right)^2 + R(r)^2 \left(\frac{d\theta}{d\tau}\right)^2 + R(r)^2 \sin^2\theta \left(\frac{d\phi}{d\tau}\right)^2 \right) \quad (18)$$

Here,  $\tau$  is an affine parameter along the geodesics. The canonical mometa corresponding to each coordinate is given as,

$$p_t = \frac{d\mathcal{L}}{d\dot{t}} = f\dot{t} \quad (19)$$

$$p_r = -\frac{d\mathcal{L}}{d\dot{r}} = \frac{\dot{r}}{f} \quad (20)$$

$$p_\theta = -\frac{d\mathcal{L}}{d\dot{\theta}} = R(r)^2\dot{\theta} \quad (21)$$

$$p_\phi = -\frac{d\mathcal{L}}{d\dot{\phi}} = R(r)^2\sin^2\theta\dot{\phi} \quad (22)$$

Since the GMGHS black hole have two Killing vectors  $\partial_t$  and  $\partial_\phi$ , there are two constants of motion which can be labeled as  $E$  and  $L$  given as,

$$p_t = f\dot{t} = E \quad (23)$$

$$p_\phi = R(r)^2\sin^2\theta\dot{\phi} = L \quad (24)$$

Furthermore, from the Euler-Lagrangian equation of motion,

$$\frac{d}{d\tau} \left( \frac{d\mathcal{L}}{d\dot{\theta}} \right) - \frac{d\mathcal{L}}{d\theta} \Rightarrow -\frac{dp_\theta}{d\tau} - \frac{d\mathcal{L}}{d\theta} = 0 \Rightarrow \frac{d(-R(r)^2\dot{\theta})}{d\tau} + R(r)^2\sin\theta\cos\theta \left( \frac{d\phi}{d\tau} \right)^2 = 0 \quad (25)$$

Hence, if we choose  $\theta = \pi/2$  and  $\dot{\theta} = 0$  as the initial conditions, the eq.(25) leads to,

$$\frac{d(R(r)^2\dot{\theta})}{d\tau} = R(r)^2\ddot{\theta} + \frac{dR(r)^2}{d\tau}\dot{\theta} = 0 \quad (26)$$

Therefore,  $\ddot{\theta} = 0$ .  $\theta$  will remain at  $\pi/2$  and the geodesics will be described in an invariant plane at  $\theta = \pi/2$ . From eq.(23) and eq.(24),

$$R(r)^2\dot{\phi} = L; \quad f(r)\dot{t} = E \quad (27)$$

With  $\dot{t}$  and  $\dot{\phi}$  given by equation(27), the Lagrangian in eq.(18) simplifies to be,

$$\dot{r}^2 + f(r) \left( \frac{L^2}{R(r)^2} + h \right) = E^2 \quad (28)$$

Here,  $\mathcal{L} = h$ .  $h = 1$  corresponds to time-like geodesics and  $h = 0$  corresponds to null geodesics. For a time-like geodesic,  $\tau$  may be identified with proper time of the particle describing the geodesic. Comparing eq.(28) with  $\dot{r}^2 + V_{eff} = E^2$ , one get the effective potential, which depend on  $E$  and  $L$  as follows:

$$V_{eff} = \left( \frac{L^2}{R(r)^2} + h \right) f(r) \quad (29)$$

By eliminating the parameter  $\tau$  from the equations(27) and (28), one can get a relation between  $\phi$  and  $r$  as follows;

$$\frac{d\phi}{dr} = \frac{L}{R(r)^2} \frac{1}{\sqrt{(E^2 - V_{eff})}} \quad (30)$$

## 4 Null Geodesics in Einstein frame

In the above formalism,  $h = 0$  for null geodesics.

### 4.1 Radial null geodesics

The radial geodesics corresponds to the motion of particles with zero angular momentum ( $L = 0$ ). Hence for radial null geodesics, the effective potential,

$$V_{eff} = 0 \quad (31)$$

The two equations for  $\dot{t}$  and  $\dot{r}$  simplifies to,

$$\dot{r} = \pm E; \quad \dot{t} = \frac{E}{f(r)} \quad (32)$$

The above two equations lead to,

$$\frac{dt}{dr} = \pm \frac{1}{f(r)} = \pm \frac{1}{(1 - \frac{2m}{r})} \quad (33)$$

The above equation can be integrated to give the coordinate time  $t$  as a function of  $r$  as,

$$t = \pm \left( r + 2m \ln \left( \frac{r}{2m} - 1 \right) \right) + \text{const}_{\pm} \quad (34)$$

When  $r \rightarrow 2m$ ,  $t \rightarrow \infty$ . On the other hand, the proper time can be obtained by integrating,

$$\frac{d\tau}{dr} = \pm \frac{1}{E} \quad (35)$$

which leads to,

$$\tau = \pm \frac{r}{E} + \text{const}_{\pm} \quad (36)$$

When  $r \rightarrow 2m$ ,  $\tau \rightarrow \pm \frac{2m}{E}$ , which is finite. Hence the proper time is finite while the coordinate time is infinite. This is the same results one would obtain for the Schwarzschild black hole[8].

## 4.2 Geodesics with angular momentum ( $L \neq 0$ )

In this section, we will study the null geodesics with angular momentum.

### 4.2.1 Effective potential

In this case,

$$V_{eff} = f(r) \frac{L^2}{R(r)^2} \quad (37)$$

For  $r = 2m$ ,  $V_{eff} = 0$  and for  $r \rightarrow \infty$ ,  $V_{eff} \rightarrow 0$ . In the Fig. 1, the  $V_{eff}$  is given for various values of  $a$ . One can note that the height is higher for the string black hole in comparison to the Schwarzschild black hole.

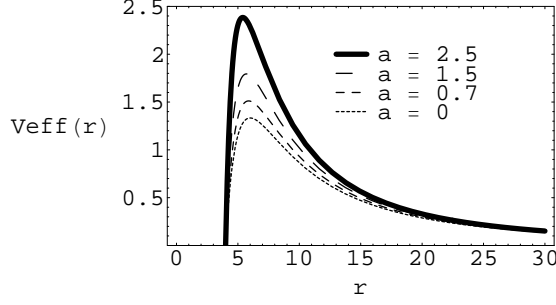


Figure 1. The graph shows the relation of  $V_{eff}$  with the parameter  $a$ . Here,  $m = 2, L = 12$

In Fig.2 the effective potential for various values of the angular momentum  $L$  is given. As expected, the effective potential is larger for large  $L$ .

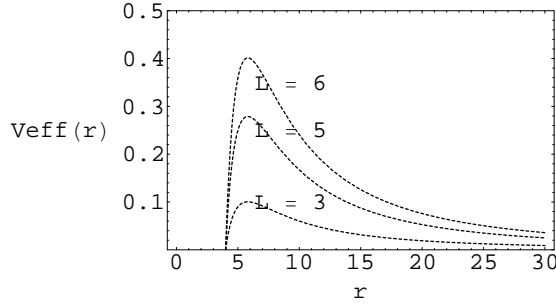


Figure 2. The graph shows the relation of  $V_{eff}$  with the angular momentum  $L$ . Here  $m = 2, a = 1.5$

Since  $\dot{r}^2/2 + V_{eff} = E^2$ , the motion of the particles depend on the energy levels. In the Fig.3, the effective potential is plotted and three energy levels,  $E_1$ ,  $E_c$  and  $E_2$  are given which corresponds to three different scenarios of motion of the particles which is described below.

**Case 1:**  $E = E_c$

Here,  $E^2 - V_{eff} = 0$  and  $\dot{r} = 0$  leading to circular orbits. However, due to the nature of the potential at  $r = r_c$ , these are unstable circular orbits which will be presented in detail in the section(4.2.3).

**Case 2:**  $E = E_2$

Here,  $E^2 - V_{eff} \geq 0$  only for  $r \leq r_A$  and  $r \geq r_P$  ( as indicated in Fig.3). Hence the motion is possible only in those regions. If the photons start at infinity, it will fall

to a minimum radius  $r_P$  and flies back to infinity. Hence the photons are deflected. If the photons start at  $r = r_A$ , they will fall into the singularity crossing the horizon at  $r = 2m$ .

**Case 3:**  $E = E_1$

Here,  $E^2 - V_{eff} \geq 0$  and  $\dot{r} > 0$  for all  $r$  values. Hence the photons coming from infinity cross the horizon at  $r = 2m$  and falls into the singularity at  $r = a$ .

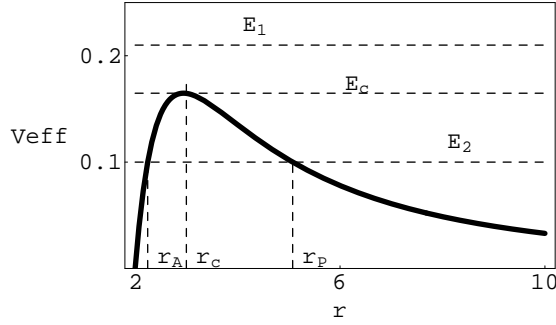


Figure 3. The graph shows the relation of  $V_{eff}$  with the energy  $E$ . Here,  $m = 1, a = 0.3$  and  $L = 2$ .

#### 4.2.2 Analysis of the geodesics with the variable $u = \frac{1}{r}$

One can also study the orbits by doing a well known change of variable  $u = \frac{1}{r}$ . Then the eq.(30) can be rewritten in terms of  $u$  and  $\phi$  as,

$$\left(\frac{du}{d\phi}\right)^2 = f(u) \quad (38)$$

where,

$$f(u) = -2amu^4 + (a + 2m)u^3 + u^2 \left( a^2 \frac{E^2}{L^2} - 1 \right) - 2a \frac{E^2}{L^2} u + \frac{E^2}{L^2} \quad (39)$$

The function  $f(u)$  for general values of  $m, a, E$  and  $L$  is given in the Fig.4.

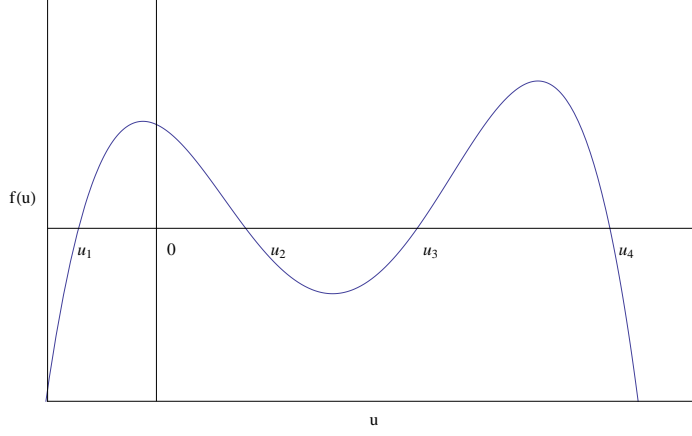


Figure 4. The graph shows the function  $f(u)$  for  $m = 0.5, a = 0.6, L = 30$  and  $E = 9$ .

When  $a \rightarrow 0$ ,  $f(u) \rightarrow 2mu^3 - u^2 + \frac{E^2}{L^2}$  as expected for the Schwarzschild black hole [8]. When  $a \rightarrow 0$ ,  $f(u)$  has maximum three real roots as described in the book by Chandrasekhar[8]. The function for  $a = 0$  is given in the Fig.5.

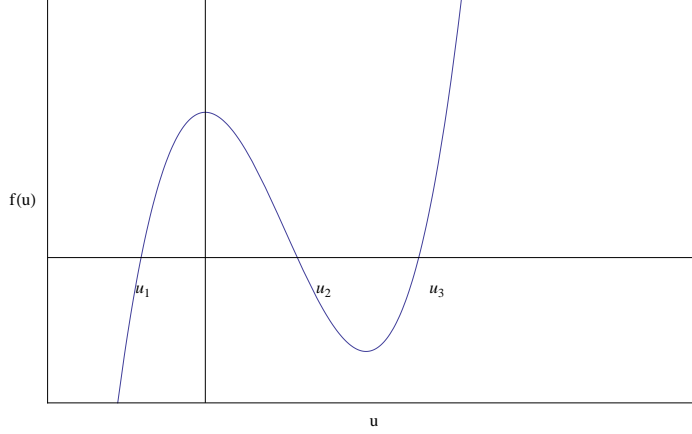


Figure 5. The graph shows the function  $f(u)$  for  $m = 0.5, a = 0, L = 30$  and  $E = 9$ .

In analyzing the null geodesics of the string black hole, it is clear that the geometry of the geodesics depends on the nature of the roots of the equation  $f(u) = 0$ . Note that for any value of the parameters in the theory  $m, a, L, E$ , the function  $f(u) \rightarrow -\infty$  for  $u \rightarrow \pm\infty$ . Also, for  $u = 0$ ,  $f(u) = +\frac{E^2}{L^2}$ . Therefore,  $f(u)$  definitely has one negative real root ( $u_1$ ). Furthermore,  $f(u)$  also has a real root at  $u_4 = 1/a$ . This can be observed by the fact that  $f(u)$  has a factor  $(-1 + au)$  as follows,

$$f(u) = \frac{(-1 + au)}{L^2} \left( E^2(-1 + au) - L^2 u^2(-1 + 2mu) \right) \quad (40)$$

Since one of the roots for  $f(u)$  is known, it is possible to write it as

$$f(u) = -2ma \left( u - \frac{1}{a} \right) g(u) \quad (41)$$

Here,  $g(u)$  is a cubic polynomial given by,

$$g(u) = (u - u_1)(u - u_2)(u - u_3) = u^3 - \frac{1}{2m}u^2 - \frac{aE^2}{2mL^2}u + \frac{E^2}{2mL^2} \quad (42)$$

The roots of  $g(u)$  are given by  $u_1, u_2$  and  $u_3$ . Since  $u_1$  is real, there are two possibilities for  $u_2$  and  $u_3$ : *either*, both are real *or* they are a complex-conjugate pair. The sum and the products of the roots  $u_1, u_2$  and  $u_3$  of the polynomial  $g(u)$  are related to the coefficients of  $g(u)$  as[19],

$$u_1 + u_2 + u_3 = \frac{1}{2m} \quad (43)$$

$$u_1 u_2 u_3 = -\frac{E^2}{2mL^2} \quad (44)$$

As discussed earlier,  $u_1$  is real and negative. Therefore, the roots  $u_2, u_3$  has to be positive if they are real. This conclusion comes from observing the signs of the eq.(43) and eq.(44). Overall, the polynomial  $f(u)$  has a negative( $u_1$ ) and a positive( $u_4$ ) real root always. The other two roots ( $u_2, u_3$ ) will be either real or complex-conjugate. If they are real, then they will be positive. Also, if they are real, they could be degenerate roots as well.

#### 4.2.3 Case 1: Circular orbits

The conditions for the circular orbits are,

$$\dot{r} = 0 \Rightarrow V_{eff} = E_c^2 \quad (45)$$

and

$$\frac{dV_{eff}}{dr} = 0 \quad (46)$$

From eq.(46), one get two solutions for circular orbit radius  $r$  as,

$$r_{\pm} = \frac{1}{4} \left( a + 6m \pm \sqrt{36m^2 - 20am + a^2} \right) \quad (47)$$

$r_+ \geq 2m$  and  $r_- \leq 2m$ . This is graphically represented in Fig.6.

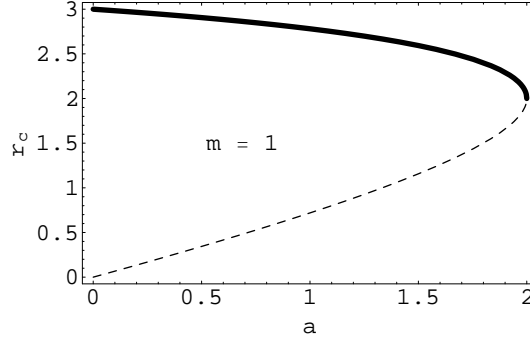


Figure 6. The graph shows the relation of  $r_{\pm}$  with  $a$ . The dark curve is for  $r_+$  and the dashed curve is for  $r_-$ . Here  $m = 1$ .

Also,  $r_{\pm}$  are real when  $a \leq 2m$  or  $a \geq 18m$ . Since we have assumed  $a < 2m$  for the purpose of the work in this paper, radius of the circular orbit that we are interested is  $r_+$  which we will rename as  $r_c$  during the rest of the paper. Hence,

$$r_c = \frac{1}{4} \left( a + 6m + \sqrt{36m^2 - 20am + a^2} \right) \quad (48)$$

The circular orbits at  $r = r_c$  are unstable due to the nature of the potential at  $r = r_c$ . The hypersurface at  $r = r_c$  is known as the “photon sphere”. For a detailed discussion about photon spheres see the paper by Claudel et.al[20]. When  $a \rightarrow 0$ ,  $r_c \rightarrow 3m$  which is the radius of the unstable circular orbit of the Schwarzschild black hole[8].

The radius of the circular orbit  $r_c$  in eq.(48) is independent of  $E$  and  $L$ . However, they are related to each other from eq.(45) as,

$$\frac{E_c^2}{L_c^2} = \frac{f(r_c)}{R^2(r_c)} = \frac{(r_c - 2m)}{r_c^2(r_c - a)} = \frac{1}{D_c^2} \quad (49)$$

Here,  $D_c$  is the impact parameter at the critical stage. When  $a \rightarrow 0$ ,  $D_c^2 \rightarrow 27m^2$  which is the impact parameter for the unstable circular orbits of the Schwarzschild black hole [8].

One can also study the circular orbits using the function  $f(u)$  introduced in section(4.2.2). Circular orbits exists when  $f(u)$  has a real degenerate root( $u_2 = u_3 = u_c$ ). Hence,  $f(u)$  can be written as,

$$f(u) = -2ma(u - u_c)^2(u - \frac{1}{a})(u - u_1) \quad (50)$$

Here,  $u_c = \frac{1}{r_c}$ , where  $r_c$  is given by eq.(48). From eq.(43),

$$u_1 = \frac{1}{2m} - 2u_c \quad (51)$$

The graph for  $f(u)$  for this particular case is given in the Fig. 7.

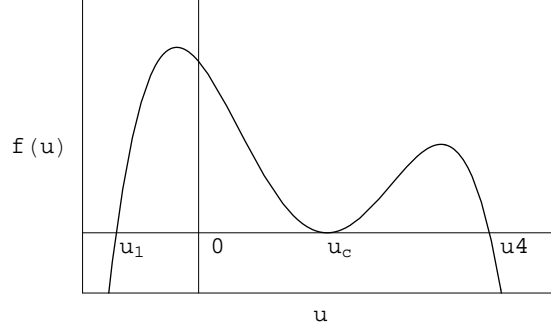


Figure 7. The graph shows the function  $f(u)$  for  $m = 0.5, E = 9, a = 0.6, L = 17.7842$ . Note that due to the degenerate roots,  $E$  and  $L$  are related by the eq.(49).

For a null geodesic arriving from infinity and approaching the black hole, the motion is given by the region from  $u \rightarrow 0 (r \rightarrow \infty)$  to  $u \rightarrow u_c (r \rightarrow r_c)$ . This is given by the region from  $u = 0$  to  $u = u_c$  in Fig. 7. During this region, since  $u \geq 0$  and  $u_1 \leq 0$ ,  $u - u_1 > 0$ . Also,  $(u_4 - u) = (\frac{1}{a} - u) > 0$  for obvious reasons. Therefore,  $f(u) > 0$  for  $0 \leq u \leq u_c$ . Hence

$$\left(\frac{du}{d\phi}\right) = \pm \sqrt{f(u)} \quad (52)$$

The “+” sign will be chosen without loss of generality. One can integrate the equation,  $\frac{du}{\sqrt{f(u)}} = d\phi$  to get a relation between  $u$  and  $\phi$  as,

$$u = \frac{\frac{u_4}{c_0^2} \tanh^2\left(\frac{\phi - \phi_0}{a_0}\right) + u_1}{1 + \frac{1}{c_0^2} \tanh^2\left(\frac{\phi - \phi_0}{a_0}\right)} \quad (53)$$

Here,  $\phi_0$  is a constant of integration chosen such that when  $u = 0$ ,  $\phi = 0$ .  $a_0$  and  $c_0$  are constants.  $\phi_0$ ,  $a_0$  and  $c_0$  are given by,

$$\phi_0 = -a_0 \arctan\left(\sqrt{-\frac{u_1}{u_4}} c_0\right) \quad (54)$$

$$a_0 = \sqrt{\frac{2}{ma}} \frac{1}{\sqrt{(u_4 - u_c)(u_c - u_1)}} \quad (55)$$

$$c_0 = \sqrt{\frac{u_4 - u_c}{u_c - u_1}} \quad (56)$$

In the Fig. 8, the polar plot of the null geodesics are given for photons arriving from infinity and having an unstable circular orbit at  $r = r_c$ .

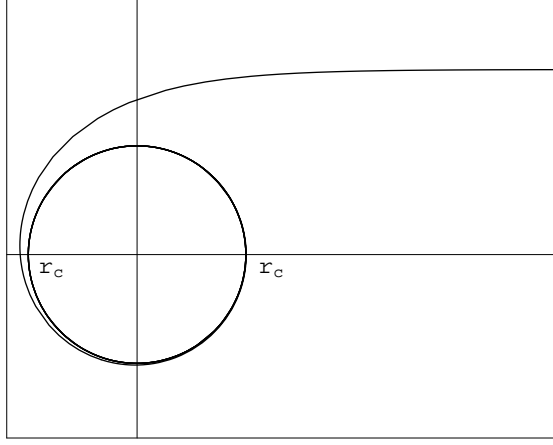


Figure 8. The polar plot shows the critical null geodesics approaching the black-hole from infinity. The geodesics have an unstable circular orbit at  $r = r_c$ . Here,  $m = 1$ ,  $a = 0.2$  and  $r_c = 2.9651$ .

### The Time Period

The time period for circular orbits can be calculated for proper time as well as coordinate time with  $\phi = 2\pi$ . From eq.(27),

$$T_\tau = \frac{2\pi r_c(r_c - a)}{L} \quad (57)$$

From combining the two equations in eq.(27),

$$T_t = \frac{2\pi R(r_c)}{\sqrt{f(r_c)}} = \frac{2\pi \sqrt{r_c^2(r_c - a)}}{\sqrt{r_c - 2m}} \quad (58)$$

One can compute  $T_\tau$  and  $T_t$  for the Schwarzschild black hole by taking the limit  $a \rightarrow 0$  which results in the following,

$$T_{t,Sh} = 3\sqrt{3}m \quad (59)$$

and

$$T_{\tau,Sh} = \frac{2\pi(3m)^3}{L} \quad (60)$$

By observing the graphs of the time periods, it is clear that the periods for the Schwarzschild black hole is larger in comparison with the string black hole.

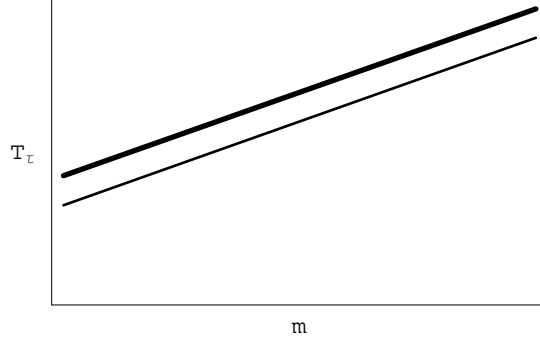


Figure 9. The graph shows the relation of  $T_\tau$  with the mass  $m$ . The dark curve is for  $T_{\tau,Sh}$  and the light curve is for  $T_{\tau,String}$ . Here,  $a = 1$  and  $L = 1$ .

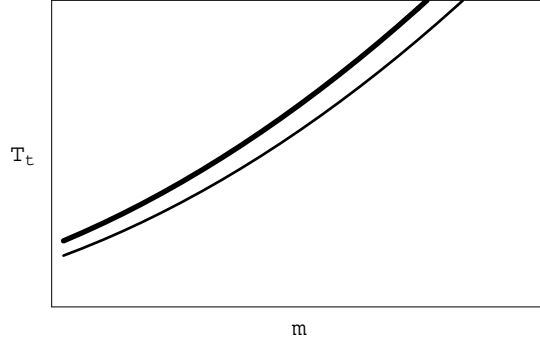


Figure 10. The graph shows the relation of  $T_t$  with  $m$ . The dark curve is for  $T_{t,Sh}$  and the light curve is for  $T_{t,String}$ . Here  $a = 1$  and  $L = 1$ .

### The Cone of avoidance

One can define the “cone of avoidance” similar to what is described in [8] as follows.

The null rays described by the eq.(53), passing a point in the space-time forms the generators of the cone. Let  $\Psi$  denote the half-angle of the cone directed towards the black hole at large distances. Then,

$$\cot\Psi = +\frac{d\bar{r}}{R(r)d\phi} \quad (61)$$

Here,  $\bar{r}$  is the proper length along the generators of the cone. Hence,

$$d\bar{r} = \frac{1}{\left(1 - \frac{2m}{r}\right)} dr \quad (62)$$

After substitution,  $\cot\Psi$  becomes,

$$\cot\Psi = \frac{1}{\sqrt{\left(1 - \frac{2m}{r}\right)r(r-a)}} \frac{dr}{d\phi} \quad (63)$$

One can rewrite the above equation in terms of  $u = \frac{1}{r}$  and replace  $\frac{du}{d\phi}$  with  $\sqrt{f(u)}$  given in eq.(52) to obtain,

$$\cot\Psi = \frac{\sqrt{f(u)}}{\sqrt{u^2(1-2mu)(1-au)}} \quad (64)$$

Hence the cone of avoidance for the the null geodesics with the critical impact parameter with the solution given in eq.(53) can be written as,

$$\tan\Psi = \frac{\sqrt{u^2(1-2mu)}}{\sqrt{2m(u-u_c)^2(u-u_1)}} \quad (65)$$

From the above equation, it follows that,

$$\text{for} \quad u \rightarrow u_c (r \rightarrow r_c), \quad \Psi = \pi/2 \quad (66)$$

and,

$$\text{for} \quad u \rightarrow 0 (r \rightarrow \infty), \quad \Psi \approx \sqrt{-\frac{1}{2mu_1u_c^2}} \left(\frac{1}{r}\right) \quad (67)$$

Note that  $u_1 < 0$  which makes  $\Psi$  real in eq.(67). If we take the limit  $a \rightarrow 0$ , the above equation,  $\Psi$  approaches  $3\sqrt{3}m \left(\frac{1}{r}\right)$  which is the value for the Schwarzschild black hole given in[8].

#### 4.2.4 Case 2 and 3: Unbounded orbits

##### Case 2 : $\mathbf{E = E_2}$

Here, we will study Case 2 given in the section(4.2.1). In this case,  $f(u) = 0$  has four real roots. Therefore, the motion is possible in two regions given as 1 and 2 in the Fig 11.

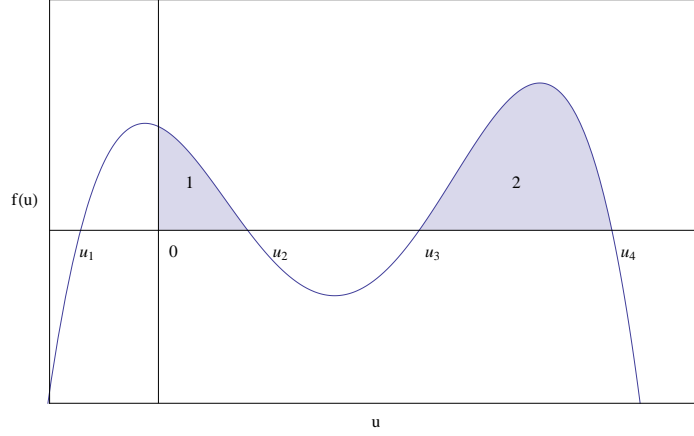


Figure 11. The graph shows the function  $f(u)$  when it has four real roots.

If the particle starts at infinity ( $r = \infty$  or  $u = 0$ ), it will fall up to  $u_2$  (or  $r = r_P$ ) and fly away to infinity. Since  $\frac{du}{\sqrt{f(u)}} = d\phi$ , one can integrate both sides to get  $\phi$  in terms of Jacobi elliptic integral  $\mathcal{F}(\xi, y)$  as,

$$\phi = \frac{-2i\mathcal{F}(\xi, y)}{\sqrt{2ma(u_4 - u_1)(u_3 - u_2)}} + \text{constant} \quad (68)$$

Here,

$$\sin \xi = \sqrt{\frac{(u - u_2)(u_4 - u_1)}{(u - u_1)(u_4 - u_2)}} \quad (69)$$

$$y = \frac{(u_3 - u_1)(u_4 - u_2)}{(u_3 - u_2)(u_4 - u_1)} \quad (70)$$

The angle  $\phi$  is chosen such that for  $u = u_2$ ,  $\phi = 0$ . Hence the integration constant is zero. The corresponding motion is given in Fig 12.

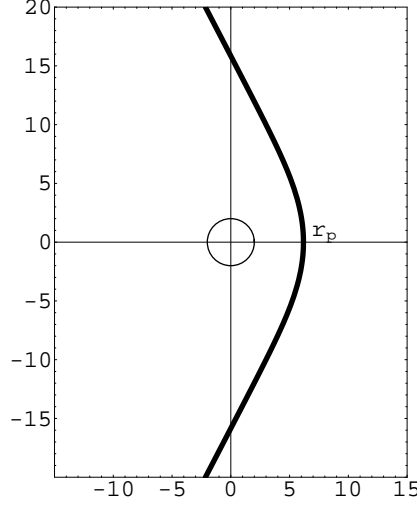


Figure 12. The polar plot shows the null geodesics approaching the black hole from infinity. The geodesics Here,  $m = 1, a = 0.6, L = 100$  and  $E = 14$ .

The other unbounded orbit for  $E = E_2$  corresponds to the motion starting from  $r = r_A$  (or  $u = u_3$ ). Here, the particle will fall into the singularity at  $r = a$  (or  $u = u_4$ ) crossing the horizon. In this case, the solutions for  $\phi$  is similar as in eq.(68). Therefore, we will omit the explicit expressions for the  $\phi$  in this case. The integration constant is chosen such that  $\phi = 0$  when  $u = u_3$ . In this case, the integration constant is not zero. The corresponding motion is given in Fig 13.

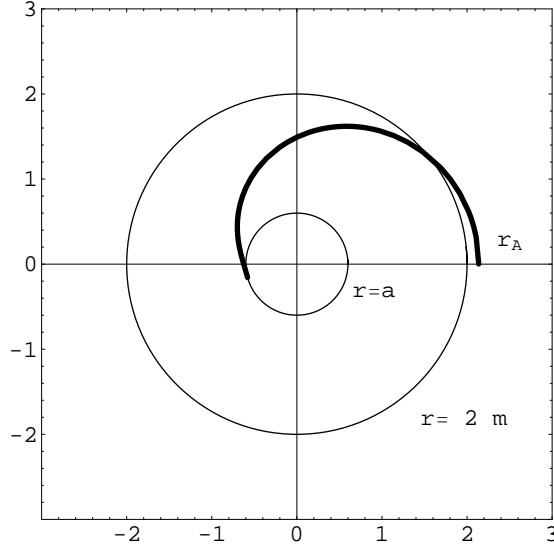


Figure 13. The polar plot shows the null geodesics falling into the black hole from

$r = r_A$ . Here,  $m = 1, a = 0.6, L = 100$  and  $E = 14$ .

**Case 3 :  $E = E_1$**

Here, we will study the Case 3 given in the section(4.2.1). In this case,  $f(u) = 0$  has only two real roots as given in Fig 14.

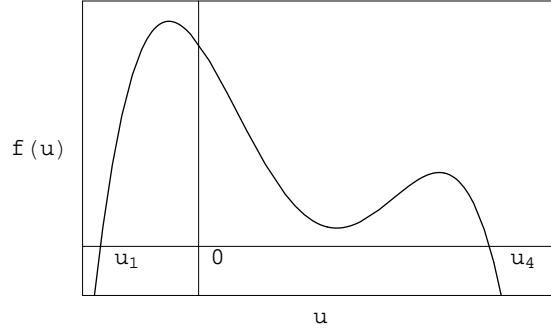


Figure 14. The graph shows the function  $f(u)$  when it has only two real roots. Therefore, the motion is possible in all regions from infinity to the singularity. The integration of  $\frac{du}{\sqrt{f(u)}} = d\phi$  gives the same results for  $\phi$  as in eq.(68). However, in this case,  $u_2$  and  $u_3$  are both imaginary and  $u_1$  and  $u_4$  are real. The integration constant is also imaginary. But,  $\phi$  is real. The corresponding motion is given in Fig 15.

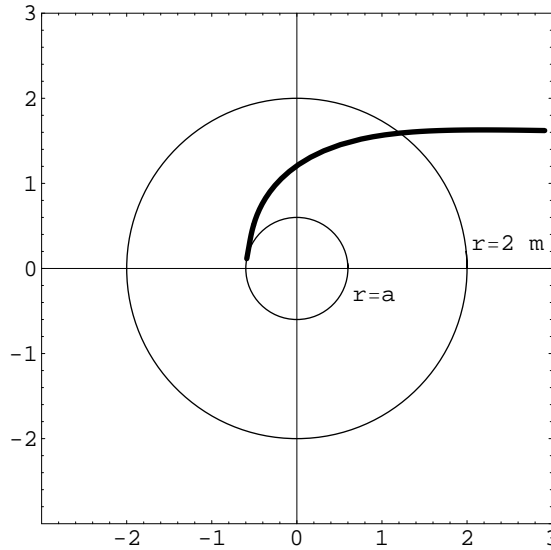


Figure 15. The polar plot shows the null geodesics approaching the black hole from infinity. The geodesics Here,  $m = 1, a = 0.6, L = 15$  and  $E = 10$ .

## 5 Geodesics in String Frame

The approach in deriving the geodesics for the string frame is similar to the approach for the geodesics in the Einstein frame. First, let us rewrite the metric in the string frame as,

$$ds^2 = -f(r)dt^2 + g(r)^{-1}dr^2 + r^2(d\theta^2 + \sin^2(\theta)d\phi^2) \quad (71)$$

Here,

$$f(r) = \frac{\left(1 - \frac{2m}{r}\right)}{\left(1 + \frac{2m \sinh^2(\alpha)}{r}\right)^2} = \frac{\left(1 - \frac{2m}{r}\right)}{\left(1 + \frac{2b}{r}\right)^2} \quad (72)$$

$$g(r) = \left(1 - \frac{2m}{r}\right) \quad (73)$$

$$b = m \sinh^2(\alpha) \quad (74)$$

Equations governing the geodesics in this space-time can be derived from the Lagrangian equation,

$$\mathcal{L} = -\frac{1}{2} \left( -f(r) \left( \frac{dt}{d\tau} \right)^2 + \frac{1}{g(r)} \left( \frac{dr}{d\tau} \right)^2 + r^2 \left( \frac{d\theta}{d\tau} \right)^2 + r^2 \sin^2 \theta \left( \frac{d\phi}{d\tau} \right)^2 \right) \quad (75)$$

Here,  $\tau$  is an affine parameter along the geodesics. The canonical momenta corresponding to each coordinate is,

$$p_t = \frac{d\mathcal{L}}{d\dot{t}} = f\dot{t} \quad (76)$$

$$p_r = -\frac{d\mathcal{L}}{d\dot{r}} = \frac{\dot{r}}{g} \quad (77)$$

$$p_\theta = -\frac{d\mathcal{L}}{d\dot{\theta}} = r^2\dot{\theta} \quad (78)$$

$$p_\phi = -\frac{d\mathcal{L}}{d\dot{\phi}} = r^2 \sin^2 \theta \dot{\phi} \quad (79)$$

Since the GMGHS black hole have two Killing vectors  $\partial_t$  and  $\partial_\phi$ , there are two constants of motion which can be labeled as  $E$  and  $L$  given as,

$$p_t = f\dot{t} = E \quad (80)$$

$$p_\phi = r^2 \sin^2 \theta \dot{\phi} = L \quad (81)$$

Furthermore, from the Euler-Lagrangian equation of motion,

$$\frac{d}{d\tau} \left( \frac{d\mathcal{L}}{d\dot{\theta}} \right) - \frac{d\mathcal{L}}{d\theta} = 0 \Rightarrow -\frac{dp_\theta}{d\tau} - \frac{d\mathcal{L}}{d\theta} = 0 \Rightarrow -\frac{d(r^2\dot{\theta})}{d\tau} + r^2 \sin \theta \cos \theta \left( \frac{d\phi}{d\tau} \right)^2 = 0 \quad (82)$$

Hence, if we choose  $\theta = \pi/2$  and  $\dot{\theta} = 0$  as the initial conditions, the eq.(82) leads to,

$$r^2\ddot{\theta} + \frac{dr^2}{d\tau}\dot{\theta} = 0 \quad (83)$$

Therefore,  $\ddot{\theta} = 0$ .  $\theta$  will remain at  $\pi/2$  and the geodesics will be described in an invariant plane at  $\theta = \pi/2$ . From eq.(80) and eq.(81),

$$r^2\dot{\phi} = L; \quad f(r)\dot{t} = E \quad (84)$$

With  $\dot{t}$  and  $\dot{\phi}$  given by equation(84), the Lagrangian in eq.(75) simplifies to be,

$$\dot{r}^2 + g(r) \left( \frac{L^2}{r^2} + h \right) = E^2 \frac{g(r)}{f(r)} \quad (85)$$

We have replaced  $2\mathcal{L} = h$ .  $h = 1$  corresponds to time-like geodesics and  $h = 0$  corresponds to null geodesics. For a time-like geodesics,  $\tau$  may be identified with proper time of the particle describing the geodesics. Comparing eq.(85) with  $\dot{r}^2/2 + V_{eff} = 0$ , one get the effective potential, which depend on  $E$  and  $L$  as follows:

$$V_{eff} = \left( \frac{L^2}{r^2} + h \right) g(r) - E^2 \frac{g(r)}{f(r)} \quad (86)$$

By eliminating the parameter  $\tau$  from the equations (84) and (85), one can get a relation between  $\phi$  and  $r$  as follows;

$$\frac{d\phi}{dr} = \frac{L}{r^2} \frac{1}{\sqrt{-V_{eff}}} \quad (87)$$

## 6 Null Geodesics in String frame

In the above formalism,  $h = 0$  for null geodesics.

### 6.1 Radial null geodesics

The radial geodesics corresponds to the motion of particles with zero angular momentum ( $L = 0$ ). Hence for radial null geodesics, the effective potential,

$$V_{eff} = -E^2 \frac{g(r)}{f(r)} \quad (88)$$

The two equations for  $\dot{t}$  and  $\dot{r}$  simplifies to,

$$\dot{r} = \pm \sqrt{\frac{g}{f}} E = \pm E \left( 1 + \frac{2b}{r} \right) \quad (89)$$

$$\dot{t} = \frac{E}{f(r)} = E \frac{(1 + \frac{2b}{r})^2}{(1 - \frac{2m}{r})} \quad (90)$$

The above two equations lead to,

$$\frac{dt}{dr} = \pm \frac{1}{\sqrt{g(r)f(r)}} = \pm \frac{(1 + \frac{2b}{r})}{(1 - \frac{2m}{r})} \quad (91)$$

The above equation can be integrated to give the coordinate time  $t$  as a function of  $r$  as,

$$t = \pm \left( r + (2m + 2b) \ln \left( \frac{r}{2m} - 1 \right) \right) + const_{\pm} \quad (92)$$

When  $r \rightarrow 2m$ ,  $t \rightarrow \infty$ . On the other hand, the proper time can be obtained by integrating,

$$\frac{d\tau}{dr} = \pm \frac{1}{E(1 + \frac{2b}{r})} \quad (93)$$

which leads to,

$$\tau = \pm \frac{1}{E} (r - 2b \ln(2b + r)) + const_{\pm} \quad (94)$$

When  $r \rightarrow 2m$ ,  $\tau \rightarrow \pm(2m - 2b \ln(2b + 2m))/E$ , which is finite. Hence the proper time is finite while the coordinate time is infinite. This is similar to what was obtained in the Einstein frame.

## 6.2 Geodesics with angular momentum ( $L \neq 0$ )

In this section, we will study the null geodesics with angular momentum.

### 6.2.1 Effective potential

In this case,

$$V_{eff} = g(r) \frac{L^2}{r^2} - E^2 \frac{g(r)}{f(r)} \quad (95)$$

In the Fig. 16, the  $V_{eff}$  is given for various values of  $b$ . One can note, that the height is lower for the string black hole in comparison to the Schwarzschild black hole.

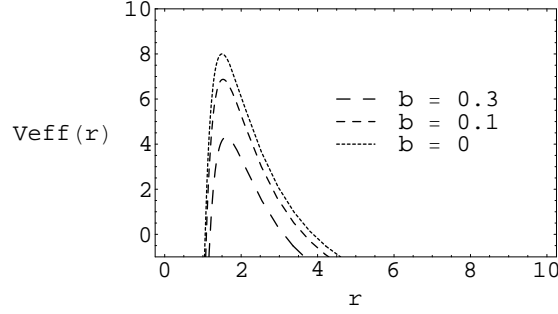


Figure 16. The graph shows the relation of  $V_{eff}$  with the parameter  $b$ . Here,  $m = 0.5, L = 12$  and  $E = 2$ .

### 6.2.2 Circular orbits

The conditions for the circular orbits are,

$$\dot{r} = 0 \Rightarrow V_{eff} = 0 \quad (96)$$

and

$$\frac{dV_{eff}}{dr} = 0 \quad (97)$$

From eq.(97), one get a solution for circular orbit radius  $r$  as,

$$r_c = \frac{1}{2} \left( 3m + \sqrt{8bm + 9m^2} \right) \quad (98)$$

The circular orbits at  $r = r_c$  are unstable due to the nature of the effective potential at  $r = r_c$ . The radius of the circular orbit is independent of  $E$  and  $L$ . However, they are related to each other from eq.(96) as,

$$\frac{E_c^2}{L_c^2} = \frac{f(r_c)}{r_c^2} = \frac{(r_c - 3m)}{2br_c(r_c + 2b)} \quad (99)$$

When  $b \rightarrow 0$ ,  $r_c \rightarrow 3m$  which is the radius of the unstable circular orbit of the Schwarzschild black hole[8].

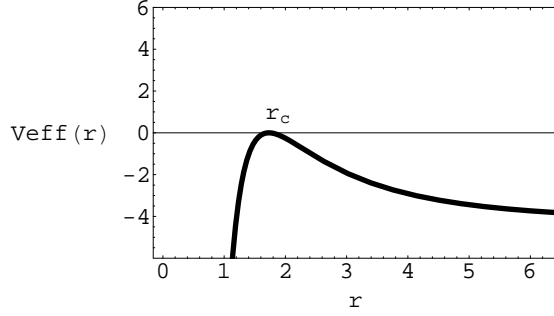


Figure 17. The graph shows  $V_{eff}$ . Here,  $m = 0.5, b = 0.4$  and  $E = 2$ . The corresponding  $L = 7.79$  and  $r_c = 1.73$ .

One can also study the orbits by doing a well known change of variable  $u = \frac{1}{r}$ . Then the eq.(87) can be rewritten in terms of  $u$  and  $\phi$  as,

$$\left(\frac{du}{d\phi}\right)^2 = f(u) \quad (100)$$

where,

$$f(u) = 2mu^3 + u^2 \left(-1 + 4b^2 \frac{E^2}{L^2}\right) + 4b \frac{E^2}{L^2} u + \frac{E^2}{L^2} \quad (101)$$

In analyzing the string black hole null geodesics, it is clear that the geometry of the geodesics depends on the nature of the roots of the equation  $f(u) = 0$ . Note that for any value of the parameters  $m, b, L, E$ , the function  $f(u) \rightarrow \infty$  for  $u \rightarrow +\infty$  and  $f(u) \rightarrow -\infty$  for  $u \rightarrow -\infty$ . Also, for  $u = 0$ ,  $f(u) = +\frac{E^2}{L^2}$ . Therefore,  $f(u)$  definitely has one negative real root ( $u_1$ ). Since  $f(u)$  is a cubic polynomial, one can rewrite it as,

$$f(u) = 2m(u - u_1)(u - u_2)(u - u_3) \quad (102)$$

The roots of  $f(u)$  are given by  $u_1, u_2$  and  $u_3$ . Since  $u_1$  is real, there are two possibilities for  $u_2$  and  $u_3$ : *either*, both are real *or* they are a complex-conjugate pair. The sum and the products of the roots  $u_1, u_2$  and  $u_3$  of the polynomial  $f(u)$  are related to the coefficients of  $g(u)$  as [19],

$$u_1 + u_2 + u_3 = \frac{1}{2m} - \frac{2b^2 E^2}{m L^2} \quad (103)$$

$$u_1 u_2 u_3 = -\frac{E^2}{2m L^2} \quad (104)$$

As discussed earlier,  $u_1$  is real and negative. Therefore, both roots  $u_2, u_3$  will be either positive or negative if they are real. This conclusion comes from observing the sign of the eq.(104). If they are real, then they could be degenerate roots as well as given in Fig. 20. The function  $f(u)$  for general values of  $m, a, E, L$  is given in the Fig.18.

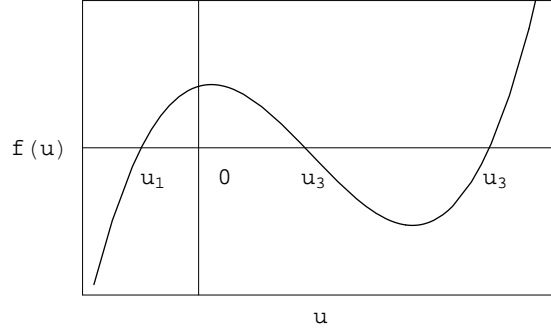


Figure 18. The graph shows the function  $f(u)$  for  $m = 0.5, b = 0.4, E = 2$  and  $L = 9.8$ .

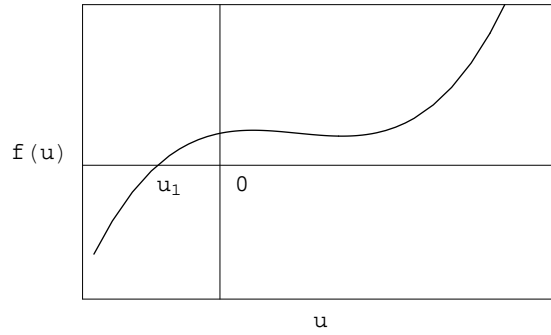


Figure 19. The graph shows the function  $f(u)$  for  $m = 0.5, b = 0.4, E = 2$  and  $L = 5.7$ .

When  $a \rightarrow 0$ ,  $f(u) \rightarrow 2mu^3 - u^2 + \frac{E^2}{L^2}$  as expected for the Schwarzschild black hole[8].

Circular orbits exists when  $f(u)$  has real degenerate roots ( $u_2 = u_3 = u_c$ ). The graph for this particular case is given in the Fig.20.

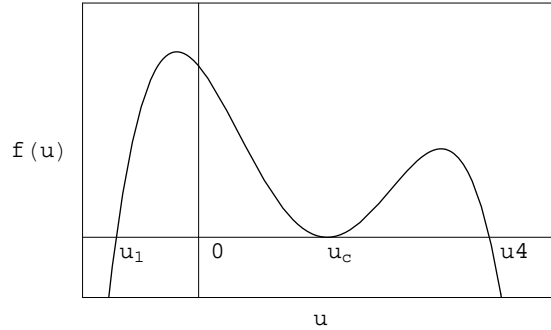


Figure 20. The graph shows the function  $f(u)$  for  $m = 0.5, b = 0.4, E = 2$  and  $L = 7.79$ .  $u_c = 0.578$ . Note that due to the degenerate roots,  $E$  and  $L$  are related by

the eq.(99).

Hence,  $f(u)$  can be written as,

$$f(u) = 2m(u - u_c)^2(u - u_1) \quad (105)$$

Here,  $u_c = \frac{1}{r_c}$ , where  $r_c$  is given by eq.(98). From eq.(103),

$$u_1 = \frac{1}{2m} - 2u_c - \frac{2b^2 E_c^2}{m L_c^2} \quad (106)$$

For a null geodesic arriving from infinity and approaching the black hole, the motion is given by the region from  $u \rightarrow 0 (r \rightarrow \infty)$  to  $u \rightarrow u_c (r \rightarrow r_c)$ . This is given by the region from  $u = 0$  to  $u = u_c$  in Fig.20. During this region, since  $u \geq 0$  and  $u_1 \leq 0$ ,  $u - u_1 > 0$ . Therefore,  $f(u) > 0$  for  $0 \leq u \leq u_c$ . Hence

$$\left(\frac{du}{d\phi}\right) = \pm\sqrt{f(u)} \quad (107)$$

The “+” sign will be chosen without loss of generality. One can integrate the equation,  $\frac{du}{\sqrt{f(u)}} = d\phi$  to get a relation between  $u$  and  $\phi$  as,

$$u = u_1 + (u_c - u_1)\tanh^2\left(\frac{\phi - \phi_0}{a_0}\right) \quad (108)$$

Here,  $\phi_0$  is a constant of integration chosen such that when  $u = 0$ ,  $\phi = 0$ .  $a_0$  is also a constant.  $\phi_0$  and  $a_0$  are given by,

$$\phi_0 = a_0 \arctan\left(\sqrt{\frac{u_1}{u_1 - u_c}}\right) \quad (109)$$

$$a_0 = -\sqrt{\frac{2}{m(u_c - u_1)}} \quad (110)$$

In the Fig.21, the polar plot of the null geodesics are given for photons arriving from infinity and having an unstable circular orbit at  $r = r_c$ .

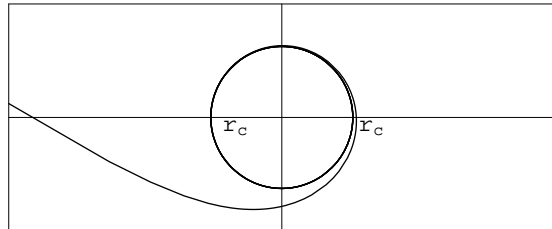


Figure 21. The polar plot shows the critical null geodesics in the string frame approaching the black hole from infinity. The geodesics have an unstable circular orbit at  $r = r_c$ . Here,  $m = 1$ ,  $b = 0.2$  and  $r_c = 3.1279$ .

## 7 Conclusions

We have studied the null geodesics of the static charged black hole in heterotic string theory. The equations for the geodesics were solved exactly for various values of energy and angular momentum of the photons. In the Einstein frame, all possible motions were presented. The circular orbits were shown to be unstable. In comparison, the circular orbits of the Reissner-Nordström black hole which is the charged black hole in general relativity is also shown to be unstable as worked out by Chandrasekhar[8]. The circular orbit of the geodesics in the string frame is also studied in detail in this paper. Since the null geodesics do not change under conformal transformations, the circular orbits in both frames are expected to be similar which is shown analytically in this paper.

There are several avenues one would like to continue this work. Decanini et.al[21] wrote an interesting paper studying nonlinear dispersion relations and the damping of the “surface waves” lying close to unstable circular orbits of static spherically symmetric black holes. It would be interesting to study the massless wave equation around the charged string black hole in this context since there are unstable circular orbits around it as we presented here. We like to mention that the scalar field around the string black hole has been studied by Fernando and Arnold[22]. Furthermore, in another interesting paper, Cardoso et.al[23] showed relations between quasi-normal modes of a black hole and the parameters of the circular orbits of the black hole. This is another avenue to study the circular orbits we obtained of the charged string black hole.

It would be also interesting to study the motion for the naked singularity of the charged string solutions considered in this paper. The motion of test particles around the naked singularity of the Reissner-Nordström space-times have been studied by Pugliese et.al.[5].

**Acknowledgments:** This work was done during the sabbatical leave granted to the author by Northern Kentucky University. The author likes to thank Dr. Don Krug of the Mathematics Department of Northern Kentucky University for valuable discussions at the initial stage of this work.

## References

- [1] A. Sen, *Rotating charged black hole solution in heterotic string theory*, Phys. Rev. Lett. **69** (1992) 1006–1009, hep-th/9204046
- [2] A. Sen, *Black hole solution in heterotic string theory on a Torus*, Nucl. Phys. **B440** (1995) 421-440, hep-th/9411187

- [3] G.W. Gibbons & K. Maeda, *Black holes and membranes in higher dimensional theories with dilaton fields*, Nucl. Phys. **B298** (1988) 741
- [4] D. Garfinkle, G.T. Horowitz & A. Strominger, *Charged black holes in string theory*, Phys. Rev. **D43** (1991) 3140
- [5] D. Pugliese, H. Quevedo & R. Ruffini, *Circular motion of neutral test particles in Reissner-Nordström spacetime*, Phys. Rev. **D 83** (2011) 024021
- [6] D. Pugliese, H. Quevedo & R. Ruffini, *Motion of charged test particles in Reissner-Nordström spacetime*, Phys. Rev. **D 83** (2011) 104052
- [7] S. Grunau & V. Kagramanova, *Geodesics of electrically and magnetically charged test particles in Reissner-Nordström space-time: analytical solutions*, Phys. Rev. **D 83** (2011) 044009
- [8] S. Chandrasekhar, *The Mathematical Theory of Black holes*, Oxford, UK: Clarendon (1992) 646 p.
- [9] E. Hackmann, V. Kagramanova, J. Kunz, & C. Lammerzahl, *Analytic solutions of the geodesic equation in higher dimensional static spherically symmetric space-times*, Phys. Rev. **D 78** (2008) 124018
- [10] A. Dashupta, H. Nandan & S. Kar, *Kinematics of geodesics flows in stringy black hole backgrounds*, Phys. Rev. **D 79** (2009) 124004
- [11] T. Maki & K. Shiraishi, *Motion of test particles around a charged dilatonic black hole*, Class. Quantum Grav. **11** (1994) 227
- [12] K. Hioki & U. Miyamoto, *Hidden symmetries, null geodesics, and photon capture in the Sen black hole*, Phys. Rev. **D 78** (2008) 044007
- [13] P. A. Blaga & C. Blaga, *Bounded radial geodesics around a Kerr-Sen black hole*, Class. Quantum Grav. **18** (2001) 3893
- [14] A. Bhadra, *Gravitational lensing by a charged black hole of string theory*, Phys. Rev. **D 67** (2003) 103009
- [15] S. Fernando, D. Krug & C. Curry, *Geodesics in static charged black holes in 2+1 dimensions*, Gen. Relat. and Gravit. **35** (2003) 1243
- [16] P. K. Townsend, *Black Holes*, gr-qc/9707012
- [17] R. Casadio & B. Harms, *Charge dilatonic black holes: String frame vs Einstein frame*, Mod. Phys. Lett. **A 14** (1999) 1089

- [18] G.T. Horowitz, *Dark side of string theory: Black holes and black strings*, hep-th/9210119
- [19] “Handbook of Mathematical Functions”, M. Abramowitz and A. Stegun, Dover, (1977)
- [20] C.M. Claudel, K.S. Virbhadra & G. F. R. Ellis, *The geometry of photon spheres*, J. Math. Phys. **42** (2001) 818
- [21] Y. Decanini, A. Folacci & B. Raffaelli, *Unstable circular null geodesics of static spherically symmetric black holes, Regge poles and quasinormal frequencies*, Phys. Rev. **D 81** (2010) 104039, arXiv:1002.0121
- [22] S. Fernando & K. Arnolds, *Scalar perturbation of charged black holes*, Gen. Rel. and Gravit. **36** (2004) 1805, hep-th/0312041
- [23] V. Cardoso, A.S. Miranda, E. Berti, H. Witek & V.T. Zanchin, *Geodesics stability, Lyapunov exponents and quasinormal modes*, Phys.Rev. **D79** ( 2009) 064016